This is an open access article published under an ACS AuthorChoice License, which permits copying and redistribution of the article or any adaptations for non-commercial purposes.

Macromolecules

Article

pubs.acs.org/Macromolecules

Dynamics in Crystallites of Poly(ε-caprolactone) As Investigated by Solid-State NMR

Kerstin Schäler, Anja Achilles, Ruth Bärenwald, Christiane Hackel, and Kay Saalwächter*

Institut für Physik-NMR, Martin-Luther-Universität Halle-Wittenberg, Betty-Heimann-Straße 7, D-06120 Halle/Saale, Germany

ABSTRACT: We investigate the molecular dynamics within the crystallites of poly(ε-caprolactone), PCL, crystallized from the melt by means of high-field ^{13}C and low-field ^{1}H NMR spectroscopy, addressing the question of whether it can be classified as a "crystal-fixed" polymer without chain motion through the crystallites. We address fast, slow, and intermediate-regime (microseconds to milliseconds time scale) motions by means of high-resolution of ^{13}C DIPSHIFT and CODEX MAS experiments as well as low-resolution static ^{1}H FID and MSE measurements over a range of temperatures. The DIPSHIFT data provide information on motionally averaged $^{13}C-^{1}H$ dipole−dipole couplings and indicate the presence of fast (≤1 μs) methylene group librational motions within the crystalline phase, where the amplitudes increase with increasing distance from the rather rigid ester groups. The CODEX experiments, addressing slow (≥ms) local rotations of the chemical-shift anisotropy tensors, suggest the absence of slow intracrystallite chain dynamics. ^{1}H second-moment and MSE signal loss data of the crystalline fraction, along with the DIPSHIFT and CODEX data, indicate that intermediate-regime chain motions do not take place in PCL crystallites.

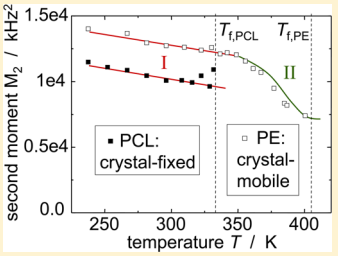

INTRODUCTION

Dynamics in semicrystalline polymers may take place within the mobile-amorphous domains, the crystalline lamellae, and interphase regions with rates from less than 1 Hz up to THz. These microscopic dynamical processes are relevant with regard to material design as they are related to the macroscopic polymer characteristics, such as brittleness, load capacity, mechanic moduli, creep, or drawability.[1−4] Hu and Schmidt-Rohr suggested a classification of semicrystalline polymers into (i) α_c-mobile and (ii) crystal-fixed polymers depending on the existence or absence, respectively, of a crystalline α-relaxation (the so-called α_c-process), enabling chain mobility within and through the crystallites.[3] The crystalline α-relaxation originates from jump processes involving a simultaneous rotation and translation of the helical polymer chain within a crystallite, in a way that this chain is left in a crystallographically allowed position and orientation before and after the jump motion.[3]

Such a helical jump process is known to happen for example in crystallites of poly(ethylene), PE, and has early on been observed, indirectly, in temperature-dependent ^{1}H NMR spectral second-moment (M_2) or rotating-frame $T_{1\rho}$ relaxation time measurements[5,6] and more recently directly by advanced dipolar ^{13}C NMR methods.[7,8] It should be noted that PE features an all-trans chain conformation in the crystallites, corresponding to a 2_1 helix, meaning that the jump angle equals 180°, which is the reason for the difficulties in directly observing it by NMR. Repeated flip processes may allow for chain diffusion between crystalline and amorphous regions, which can be investigated directly, and again more easily, by means of solid-state 2D exchange NMR spectroscopy.[3,9]

Importantly, α_c-mobile polymers with a low level of entanglements within the mobile-amorphous domains exhibit ultra-drawability and may be drawn into extremely strong fibers.[3] Further, the presence of an α_c process is considered very relevant for the crystallization and lamellar-thickening behavior of many polymers and the relation of these processes to the entangled state of the chains. This was, for instance, recently stressed in the context of results from large-scale computer simulations.[10]

The linear aliphatic polyamide Nylon with its long repeat unit and its polar NH and CO groups is an example of a crystal-fixed polymer.[3] Here, helical jumps would require a rather large displacement of the stem and the breaking of hydrogen bonds between the stems,[11] leading to a high energetic barrier for rotational and translational motions of the crystalline chain stems that suppresses the α_c-process. The situation seems to be unclear, however, in the case aliphatic polyesters. Despite a similar registry of the polar CO groups in neighboring stems within the crystallites that stabilizes the structure by favorable electrostatic dipolar interaction, at least certain linear aliphatic polyesters with long repeat units and an even number of methylene groups between the COO groups appear to exhibit an α_c-process, as detected mechanically in the form of a separate relaxation process (loss peak at 40 °C measured at ∼1 Hz, possibly reflecting larger-scale chain translation through the crystal rather than the molecular jump) and by NMR in the form of an additional decay of the second moment of the NMR proton line shape above 0 °C.[12]

The aliphatic polyester poly(ε-caprolactone) (PCL) with its relatively low melting point at around 60 °C is an interesting polymer with regard to industrial and medical applications because of its biodegradability, nontoxicity, good solubility and blend compatibility, and its convenient rheological and viscoelastic properties. It is in use in the form of drug delivery systems and sutures and is considered as a candidate for potential usage as scaffolds in tissue engineering.[13] As the molecular structure of

Received: July 22, 2013
Revised: August 24, 2013
Published: September 23, 2013

 © 2013 American Chemical Society dx.doi.org/10.1021/ma401532v | *Macromolecules* 2013, 46, 7818−7825

PCL resembles that of Nylon-6, presumably PCL should be crystal-fixed as well. In fact, no mechanical relaxation associated with the crystallites is reported for PCL above the glass transition temperature of the amorphous domains.[14] However, upon comparing ^{13}C chemical-shift anisotropy (CSA) patterns for PCL (M_n = 80 kg/mol) measured by NMR at 41 °C and simulated spectra for different methylene-group jump angles and motional rates, Kaji and Horii concluded on large-amplitude jump motions with angles around 60−90° of the methylene groups in the PCL crystallites in the intermediate to slow-motion regime.[15] They further concluded from their data that the carbonyl group is almost in the rigid state, with possible (fast) jumps being restricted to a < 30° angle range.

The unit cell in PCL crystallites is very similar to the one of PE,[16] meaning that the helical jump angle necessary for chain transport would have to be 180°. Therefore, the results of Kaji and Horii[15] do not imply the presence of an α_c process. Nevertheless, such pronounced local motions might well be the origin of or go along with a helical-jump motion that would have been undetectable with the methods of Kaji and Horii. Further, their results of have some preliminary character as, e.g., the temperature variation of the process was not checked. Thus, a consistent overall picture of PCL crystallite dynamics is still missing. Here, we address the question whether PCL can be classified as α_c-mobile or crystal-fixed; i.e., we will clarify whether helical jumps (or large-amplitude motions that may lead to such jumps at higher temperatures) take place within PCL crystallites.

As NMR experiments are sensitive to polymer chain mobility, they are well-suited in principle for investigations of polymer dynamics over a wide range of correlation times τ_c or motional rates $k \sim 1/\tau_c$. A variety of NMR techniques are available for studying dynamical processes. Often, these methods exploit the dependence of NMR interaction frequencies, such as the dipolar coupling strength or the anisotropy of the chemical shift, on the segmental orientation of the polymer chains. According to their rate k relative to the NMR interaction frequency ν_{NMR} (usually in the kHz range), motions are classified into fast (k > MHz), slow (several Hz up to kHz), and intermediate (kHz to MHz) motions. In this article we report on the investigation of potential PCL crystallite dynamics covering all three time regimes by means of different NMR methods, i.e., ^1H low-field free-induction decay (FID) and magic sandwich echo (MSE) measurements as well as ^{13}C high-field dipolar-chemical shift correlation (DIPSHIFT) and centerband-only detection of exchange (CODEX) experiments.

EXPERIMENTAL SECTION

Sample. Industrially produced PCL with M_n = 42.5 kg/mol and a polydispersity of 1.5 was purchased from Sigma-Aldrich. The material was crystallized once from the melt either isothermally at 45 C for several days (high-field measurements) or at room temperature (low-field measurements) and stored at room temperature before heating to the individual measurement temperatures.

^{13}C High-Field NMR Measurements. The high-field ^{13}C NMR measurements were performed at ^1H and ^{13}C Larmor frequencies of 400.16 and 100.06 MHz, respectively, on Bruker spectrometers equipped with a 4 mm double-resonance magic-angle spinning (MAS) probe at a spinning frequency of 5 kHz. For high-field measurements the sample was packed into a 4 mm ZrO_2 MAS rotor in the form of a small cylinder. A BVT3000 heater was used for temperature regulation with the bearing air as heat-transfer medium. The temperature accuracy amounted to ±1 K, and the temperature gradient over the sample was in the range of 0.5 K. The repetition delay was chosen to be 2 s.

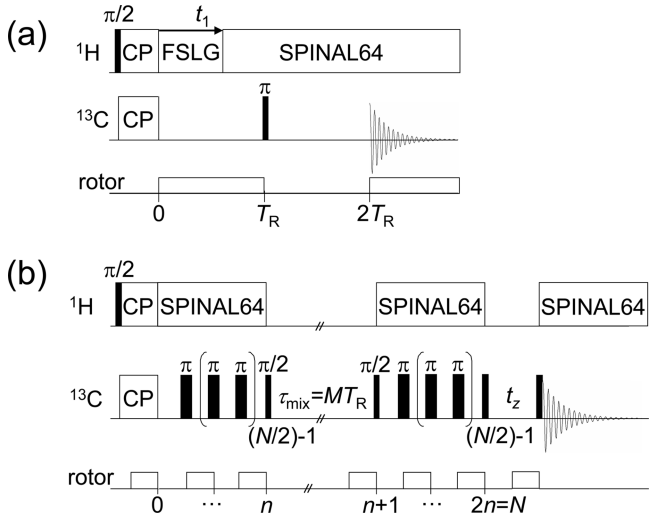

Figure 1. Pulse sequences of the (a) ^{13}C constant-time DIPSHIFT and (b) ^{13}C CODEX experiments. T_R denotes the rotor period; all other abbreviations are explained in the text.

DIPSHIFT experiments were performed using the pulse sequence shown in Figure 1a. The mode of operation of the sequence is explained in detail elsewhere.[17,18] In short, ^{13}C transverse magnetization as generated via cross-polarization (CP) selectively evolves during a variable homonuclear decoupling period t_1 under the heteronuclear $^{13}C-^1H$ dipole−dipole coupling, which is part of a Hahn echo of 2 T_R total length that compensates for chemical-shift evolution. The spectral signals, obtained after Fourier transformation of the acquired time-domain signal, thus carry a t_1-dependent intensity modulation from which the (potentially motionally averaged) $^{13}C-^1H$ dipolar coupling constant can be derived. The experiments were conducted on a Bruker Avance III spectrometer with an Oxford magnet at about 25 and 52 °C. The 90 pulse lengths were 3.5 μs and around 3.0 μs for ^1H and ^{13}C, respectively. The contact time for $^1H-^{13}C$ CP was chosen to be 0.3 ms. For heteronuclear decoupling the SPINAL64 sequence[19] was applied at a ^1H decoupling frequency of 71.5 kHz. For homonuclear decoupling, frequency-switched Lee−Goldburg (FSLG) irradiation[20] with an rf field strength of $\omega_{eff}/2\pi$ = 87.5 kHz along the effective field was used. 2048 scans were acquired for each of the 16 t_1 increments spanning one rotor period.

The CODEX pulse sequence used for investigating slow molecular jumps leading to potential PCL crystallite dynamics is shown in Figure 1b. For a detailed description of its function, we refer to previous publications.[21−23] In short, the experiment detects slow rotations of the chemical-shift anisotropy (CSA) tensor of each spectrally resolved ^{13}C resonance occurring during the mixing time τ_{mix} that can be varied in a range of milliseconds to many seconds. Before and after the mixing time, the CSA orientation is encoded via a REDOR-type 180° pulse train that recouples the CSA, whereby changes in CSA orientation lead to a signal loss. In order to account for signal decay due to simple T_1 relaxation during τ_{mix} and T_2-type relaxation during the recoupling periods, a reference intensity I_{ref} is recorded, for which τ_{mix} and a short final z filter time t_z (usually of 1 T_R length, setting the lower exchange time limit) are simply interchanged. The CODEX experiments were performed on a Bruker Avance II spectrometer with a Jastec magnet. The ^1H and ^{13}C 90 pulse lengths were 3.0 and 3.7 μs, respectively. The CP contact time was set to either 0.2 or 1.5 ms. The SPINAL64 sequence[19] was applied for heteronuclear $^1H-^{13}C$ decoupling during the recoupling and acquisition period with a decoupling frequency of 80 kHz. Exchange and reference spectra were measured for CSA recoupling durations NT_R between 0.4 and 3.2 ms with 1024 scans each and a mixing time τ_{mix} of either 100 or 200 ms. For normalization, the exchange signal intensity I was simply divided by the reference signal intensity I_{ref}.[22]

Spectral Analysis. A high-resolution ^{13}C CP spectrum of PCL measured at about 25 °C using a CP contact time of 1500 μs is shown in Figure 2. The peak assignment for the different carbon nuclei was

dx.doi.org/10.1021/ma401532v | Macromolecules 2013, 46, 7818−7825

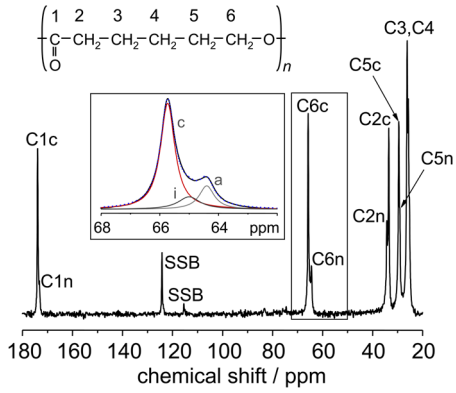

Figure 2. CP spectrum of PCL detected at about 25 °C using a CP contact time of 1500 μs. The chemical shift is given relative to TMS. The peak assignment is according to the numbering scheme shown at the top. Label parts c and n designate signal of the crystalline and the noncrystalline phases, respectively, and SSB indicates spinning sidebands. The inset shows a close-up of the C6 signal as marked by the black rectangle and includes a fit with a sum of three Lorentzian functions. The three contributions labeled c, i, and a are ascribed to the crystalline phase, the interphase, and the mobile-amorphous phase, respectively.

adopted from the literature.[24,25] The assignment of the carbon nuclei C3 and C4 in the middle of the repeat unit seems to be unclear insofar as their identity might be interchanged. For all peaks in the PCL spectrum a splitting into a crystalline-phase and a noncrystalline-phase contribution, labeled c and n, is observed due to the γ-gauche effect.[1,15] All ^{13}C spectra were analyzed via peak deconvolution by means of a fit to each peak region using a sum of two or three Lorentzian functions, with the individual fit contributions representing the signal of crystalline phase, mobile-amorphous phase, and, if necessary, an interphase (see inset of Figure 2). Phase-specific signal intensities were obtained in the form of peak areas (integrals) from the fits.

^{1}H Low-Field Time-Domain Measurements. The ^{1}H low-field time-domain measurements were carried out on Bruker minispec mq20 spectrometers with a static magnetic field of about 0.5 T and ^{1}H Larmor frequencies of 19.9 to 20.0 MHz, equipped with commercial wide-temperature range static probes. The spectrometers featured 90° pulse lengths of 1.6−3.0 μs and receiver dead times τ_{rec} of 11−15 μs. For low-field measurements the 10 mm diameter NMR sample tubes were filled to a height of about 6−8 mm with about 0.3 g of sample in the form of small pieces. The sample was placed in the center of the magnet, i.e., in the region of the highest homogeneity of the rf field. The sample temperature was regulated by means of a BVT3000 heater with air or dry nitrogen as the heat-transfer medium for heating and cooling, respectively, using active cooling for temperatures below 300 K. The temperature at the sample position could be set with an uncertainty of about 1 K and a temperature gradient over the sample of 0.5 K. All low-field time-domain NMR signals were recorded on-resonant and in full-absorption mode receiver setting, analyzing only the real part of the complex time-domain signal. The recycle delay was typically set to 1.5 s. The number of scans was varied between 16 and 256 in order to ensure a sufficiently high signal-to-noise ratio. Free induction decay (FID) signals were acquired directly after a 90° pulse (see Figure 3a) and in refocused form after application of a magic-sandwich echo (MSE) sequence[26,27] (see Figure 3b). We used a pulsed version of a mixed MSE sequence, combining a pure MSE and a Hahn echo,[28,29] in order to ensure the complete refocusing of signal dephased by homonuclear dipolar couplings and additional resonance offsets and B_0 field inhomogeneities. Details about the sequence and its mode of operation are given elsewhere.[29,30] As for short sequence lengths (n_{MSE} = 1 and τ_φ < 2.5 μs) the shape of the MSE signal of PCL closely resembles the one of the simple FID; the MSE sequence parameters were set to n_{MSE} = 1 and τ_φ = 2.2 μs in order to detect a largely undistorted time-domain signal.

Time-Domain Signal Analysis. A ^{1}H low-field time-domain NMR signal of PCL is plotted in Figure 4. It represents a superposition of

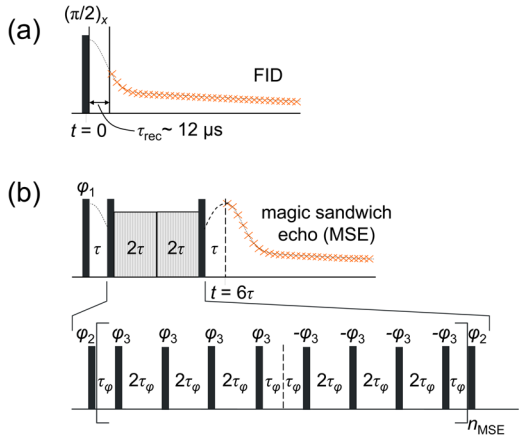

Figure 3. Schematic plot of the (a) FID and (b) MSE the pulse sequences. All pulses are 90 pulses. The signal loss in the FID during the receiver dead-time τ_{rec} is overcome by the MSE sequence. The waiting time τ in (b) is calculated as $\tau = (2\tau_{\pi/2} + 4\tau_\varphi)n_{MSE}$, with $\tau_{\pi/2}$, τ_φ, and n_{MSE} denoting the 90° pulse length, the phase-switching time, and the number of MSE cycles, respectively. The MSE phase cycle is $\varphi_1 = x\bar{x}x\bar{x}x\bar{x}x\bar{x}x$, $\varphi_2 = \bar{y}y\bar{y}y\bar{x}x\bar{x}x$, $\varphi_3 = xxxx\bar{y}y\bar{y}y\bar{y}y$.

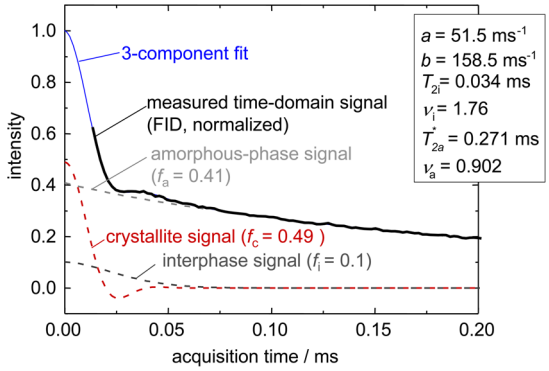

Figure 4. FID of PCL, detected after a 90° pulse at T = 30 °C, normalized and Curie-corrected to the initial intensity measured on a molten sample. The dashed lines and the solid blue line represent the phase-specific signal contributions and the complete time-domain signal, respectively, as derived in a three-component fit to the FID. Fit parameters are given in the legend.

contributions from protons in (i) rigid crystallites, (ii) liquid-like mobile-amorphous regions, and (iii) so-called "rigid-amorphous" interphase regions with intermediate mobility.

The decay time of these signal contributions is governed by the strength of the ^{1}H−^{1}H homonuclear dipolar couplings within the respective polymer phase, which is in turn influenced by the chain mobility within this phase. In the rigid crystalline phase with its rather immobile polymer chains, strong dipolar couplings between proton spins at close distances cause a rapid dephasing of transverse magnetization. Thus, a fast initial drop of the time-domain signal as well as a small oscillation is observed at acquisition times between 0.02 and 0.05 ms.[31,32] In contrast, the mobile-amorphous phase signal decays only slowly at temperatures far above T_g due to fast segmental and subsegmental motions, which average the proton dipolar couplings to a great extent. The rigid-amorphous interphase signal exhibits a decay time between the ones ascribed to the crystallites and the mobile-amorphous phase, thus indicating intermediate dipolar coupling strengths and chain mobility. For a phase-resolved signal analysis we fitted the initial 200 μs of the full time-domain signals (FID and MSE), using a weighted superposition of (i) an Abragam function $\exp\{-0.5(at)^2\}\,\sin(bt)/bt$ representing the crystallite signal, (ii) a modified exponential function $e^{-(t/T_{2a}^*)^{\nu_a}}$ characterizing the mobile-amorphous-phase

dx.doi.org/10.1021/ma401532v | Macromolecules 2013, 46, 7818−7825

signal, and (iii) a second modified exponential function $e^{-(t/T_{2i})^{\nu_i}}$ describing the interphase signal.

To ensure a stable fit with meaningful results, we restricted the values of the phase-specific shape parameters a, b, T_{2a}^*, T_{2i}, ν_a, and ν_i and weighting factors f_c, f_a, and f_i to positive values. Moreover, we used $f_c + f_a + f_i = I_{tot;T}$ as an additional constraint, with $I_{tot;T}$ denoting the total signal intensity at temperature T and acquisition time $t = 0$. As it was necessary to account for changes of the signal intensity due to different measurement temperatures, signal intensity corrections were made according to Curie's law[33] $I_{tot,T_{ref}} = I_{tot,T_{meas}}(T_{meas}/T_{ref})$, with T_{ref} and T_{meas} denoting the reference and measurement temperature. Normalizating the (unrefocused) FID signal in a way that $I_{tot;T} = 1$, the weighting factors f_c, f_a, and f_i yield the sample mass fractions.

From our data (see Figure 4), we thus derive a crystallinity of 49% and an interphase contribution of about 10%. This is consistent with the sample of Kaji and Horii[15] and previous findings in PCL samples of variable molecular weight studied previously,[34] where crystallinities always ranged around 50% and where a good correspondence was found with values determined by DSC.

RESULTS AND DISCUSSION

DIPSHIFT Measurements. DIPSHIFT experiments were used here to probe the strength of the (possibly motionally preaveraged) dipolar interaction between ^{13}C and ^{1}H nuclei of the different methylene groups within the PCL repeat unit. As the C−H dipolar interaction tensor is axially symmetric and oriented along the C−H bond, it is a viable probe for dynamic processes which change the orientation of the C−H bond with respect to the direction of the magnetic field. In this regard the DIPSHIFT experiments served to investigate fast PCL crystallite dynamics at rates k in the MHz range and above.

Figure 5 depicts the normalized signal contributions of methylene carbons in the PCL crystallites at two different temperatures as a function of the incremented time t_1 in the DIPSHIFT experiment (see Figure 1a), during which the spin system develops under the action of the heteronuclear $^{13}C-^{1}H$ dipolar coupling. We observe almost identical results for the experiments performed at 25 and 52 °C. In Figure 5, we include fits based upon a (somewhat unwieldy but straightforwardly derived) analytical formula for the DIPSHIFT signal of a CH_2 group with tetrahedral symmetry, considering only the action of the two heteronuclear dipolar couplings, the scaling factor due to the FSLG homodecoupling, a numerically calculated isotropic powder average, and an additional exponential damping term accounting for a weak apparent T_2 effect (for details see the Supporting Information in ref 17).

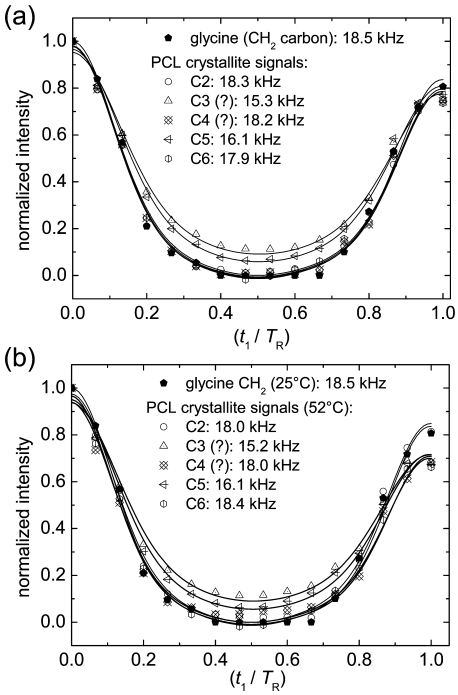

Figure 5. Crystallite signal intensities of different carbon atoms in the PCL repeat unit as a function of the normalized time t_1/T_R obtained in a DIPSHIFT experiment (see Figure 1a) at about (a) 25 °C and (b) 52 °C. The intensities are normalized to the first point at $t_1 = 0$. For a comparison, signal intensities for the carbon nucleus in the CH_2 group of the glycine reference molecule and fitted DIPSHIFT curves resulting in the indicated C−H dipolar coupling strengths are also plotted (see text).

The strength $\nu_{D,CH}$ of the C−H coupling is reflected in the modulation depth of the DIPSHIFT curves.[18] In the presence of slow dynamics with rates $k \propto 1/\tau_c \ll \nu_{D,CH}$ the full coupling strength for the static case is observed, resulting in a strong decay and low intensities at times t_1 close to half a rotor period T_R. On the other hand, fast molecular motions ($k \gg \nu_{D,CH}$) cause a partial preaveraging of couplings. Hence, the spin system effectively evolves under a reduced mean coupling strength, and the decay is slower and the minimum less deep at times $t_1 \approx T_R/2$.[18]

From fits to the data for the C2, C6, and C4 (or C3) nuclei we determine an average coupling strength $\nu_{D,CH} = 18.2 \pm 0.2$ kHz. This value is somewhat reduced as compared to the static case, $\nu_{D,CH,stat} \approx 21$ kHz, as estimated from $\nu_{D,CH,stat} = (\mu_0\hbar\gamma_C\gamma_H)/(8\pi^2 r_{C-H}^3)$[35] using the C−H distance r_{C-H} within the methylene groups of PCL, known from crystallography data,[16] and the magnetogyric ratios γ_C and γ_H of the carbon and proton spins, respectively. Figure 5 also shows data for the CH_2 group of glycine, which may be used as a rigid reference molecule. It also features a lower value of 18.5 kHz, which we attribute to uncertainties related to the scaling factor of the FSLG homodecoupling, owing to radio frequency imperfections of the used probe (in fact, with other probes we were able to reproduce the expected 21 kHz coupling for glycine). Even lower values of 16.1 and 15.3 kHz are found for the C5 and C3 (or C4) nuclei of PCL, respectively, which reside more distantly from the carboxyl groups (the lowest value for the latter in fact suggests the inverted assignment). Thus, clearly, the CH_2 groups in PLC are subject to a notable degree of preaveraging of dipolar couplings as a result of fast rotational motions at rates larger than some hundreds of kilohertz.

From the experimentally derived coupling strength $\nu_{D,CH}$, and using the glycine value as a rigid-limit reference, we obtain the following order parameters S of the motion:

$$S = \frac{\nu_{D,CH}}{\nu_{D,CH,ref}} = \frac{\nu_{D,CH}}{18.5\ \text{kHz}}$$

$$S = \begin{cases} 0.98 & \text{for C2, C6, and C4 (or C3)} \\ 0.87 & \text{for C5} \\ 0.83 & \text{for C3 (or C4)} \end{cases}$$

Assuming a two-site jump as a model for the fast rotational methylene-group vibrations according to the approach of Kaji and Horii,[15] these order parameters correspond to jump angles of less than 10° for the methylene groups close to the carboxyl groups (C2 and C6) and of 15°−25° for the more distant groups (C5 and C3 or C4) in the middle of the repeat unit (cf. Figure 13.4 in ref 36).

dx.doi.org/10.1021/ma401532v | Macromolecules 2013, 46, 7818−7825

Hence, while the carboxyl groups and the adjacent CH_2 groups, being stabilized by the dense chain packing and dipolar interactions between the chain stems within the crystallites, remain rather rigid (see ref 15), the central methylene groups perform fast larger-amplitude vibrational motions. This finding is consistent with the results of ^{13}C T_1 measurements of Kaji and Horii, who found indications of higher motional amplitudes of the methylene groups in the middle of the repeat units as compared to the positions close to the COO groups and estimated motional rates k in the range of 100 MHz.[15] Note that a similar picture was found for Nylon-66, where the methylene groups in the crystallites perform librations at rates around 0.1 THz,[37,38] while the almost rigid amide linkages act as pinning points for the neighboring methylene groups, restricting their mobility.[37]

While in the case of slow- or fast-limit chain dynamics the DIPSHIFT intensity again reaches its initial value at $t_1 = T_R$, dynamics on an intermediate time scale (k = 10−100 kHz) may lead to changes of the coupling strength during the MAS rotor period, impeding a complete signal refocusing after a full sample rotation and causing a decrease of the final intensity at $t_1 = T_R$.[18] Although glycine is rigid on an intermediate time scale, a signal decrease at $t_1 = T_R$ was also detected for its methylene carbons as a result of imperfections of the pulse sequence (see Figure 5).[39] Compared to the glycine signal intensity, the PCL data do not exhibit a significantly stronger decrease at $t_1 = T_R$ at both measurement temperatures, indicating the absence of jump or rotational motions of the methylene groups in crystalline PCL regions on an intermediate time scale. This statement will be further substantiated by the results discussed below.

CODEX Measurements. On the basis of the investigations described above, we can exclude motions in the intermediate time regime in PCL. Yet, having compared ^{13}C spectra from two-dimensional switching-angle sample-spinning (2D SASS) ^{13}C NMR measurements of melt-crystallized PCL (M_n = 80 kg/mol) at 41 °C to simulated data, Kaji and Horii concluded that jump motions of the PCL methylene groups take place around the chain axis with rather large amplitudes of about 60°−90° at rates k between 0.1 and 1 kHz, i.e., on an intermediate to slow time scale.[15] While the experiment of Kaji and Horii is sensitive to changes in the ^{13}C CSA, all our experiments are sensitive to changes in dipolar coupling tensors. Thus, the sensitivity of these individual methods for the detection of intermediate motions is different, as it depends on the ratio of the motional rate and the interaction strength probed by the individual method and on the orientation of the interaction tensor with respect to the symmetry axis of the motion. Moreover, the quantitative response to motions of a certain amplitude may differ as well.

Hence, in order to check the conclusions of Kaji and Horii concerning amplitude and time scale of motions in the PCL crystallites, we performed CODEX experiments.[21] These one-dimensional solid-state NMR exchange experiments are used for the detection and characterization of slow segmental reorientations with rates in the range of Hz to kHz by probing changes of the ^{13}C CSA. Further, recent work has shown that CODEX data also reflect motions on the intermediate time scale.[23] Thus, these results should be directly comparable to the method of Kaji and Horii.

The CODEX NT_R dependence of the normalized exchange intensity I/I_{ref} of all carbon nuclei in the repeat unit of PCL crystallites at 50 °C is depicted in Figure 6. Slow segmental or molecular reorientations would result in a decay of this exchange intensity at increasing length NT_R of the CSA recoupling periods, with T_R denoting the length of a rotor period.[21,23] No indications for signal decay were found for the PCL data, neither at 50 °C nor

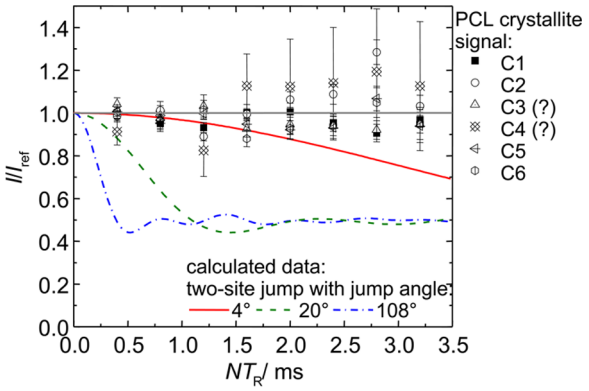

Figure 6. CODEX-NT_R dependence of the normalized crystallite-signal exchange intensity I/I_{ref} of the individual carbon atoms in the PCL repeat unit (see Figure 2), obtained from a CODEX exchange experiment at 50 °C (τ_{mix} = 100 ms, CP contact time =1500 μs). The plotted uncertainty margins result from the fits for peak deconvolution. Virtually the same results were obtained for τ_{mix} = 100 ms and also at 25 °C. For comparison, simulated curves for two-site jumps of a symmetric CSA tensor (principal values σ_{xx} = 60 ppm, σ_{yy} = 60 ppm, and σ_{zz} = 6 ppm) around its x-axis are plotted for different jump angles.

at 25 °C at two mixing times (100 and 200 ms), indicating that carbon atoms in PCL crystallites do not perform slow jumps or rotational dynamics in the range of Hz to kHz. This finding is consistent with the result of 2D exchange experiments performed by Kaji and Horii, showing the absence of motions with correlation times between 0.1 and 10 s.[15]

For comparison and illustration, in Figure 6 we also show calculated signal decays for a two-site jump motion with different jump angles, given realistic CSA principal values. As the exact values and their orientation are not known precisely, we simply use an axially symmetric tensor, even though methylene CSA tensors do exhibit a pronounced asymmetry. Nevertheless, the calculations indicate that, qualitatively, slow jumps around the chain axis differing by more than a few degrees from 0° or 180° around the chain axis can be excluded. Note that jumps among a larger number of sites would reduce the low-intensity plateau even further. The data for the carbonyl carbon (C1) in fact suggest that even slow helical jumps with angles around 180° can be excluded, as the related CSA principal values can be expected to not coincide with the symmetry axes of the all-trans chain[40] (a translation by one monomer unit would rotate the C═O vector by 180°, leading to an overall change in its CSA orientation).

Importantly, the CODEX data also hold information about intermediate-regime motions. Such motions, besides other effects such as signal losses due to the proton decoupling, T_1 relaxation and spin diffusion, cause an intensity decay of the reference signal I_{ref}.[23] Intermediate motions are best reflected in the always decaying NT_R dependence of the reference intensity I_{ref}, which reflects T_2-type effects. The decays are compared for all carbons in the crystalline-phase PCL repeat unit in Figure 7a. We notice for all methylene group carbons an equal and slightly faster decay as compared to the carbons of the COO groups, which are rather rigid on the intermediate time scale according to the data of Kaji and Horii.[15]

However, this effect originates from decoupling imperfections, which contribute significantly to the signal decay, rather than from intermediate dynamics. As the carbon nucleus in a carboxyl group resides more distantly from protons than the methylene carbons, the heteronuclear dipolar coupling interaction to be

dx.doi.org/10.1021/ma401532v | Macromolecules 2013, 46, 7818−7825

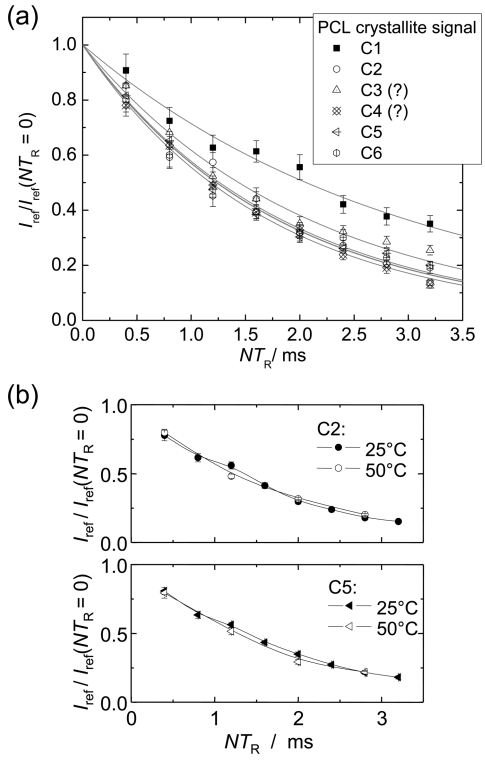

Figure 7. NT_R dependence of the crystallite signal intensities in CODEX reference experiments (τ_{mix} = 100 ms, CP contact time of (a) 200 μs and (b) 1500 μs). The data were measured at (a) 50 °C for all carbon sites in PCL (see Figure 2) and at (b) about 25 °C (open symbols) as compared to 50 °C (filled symbols) for the C2 (upper graph) and C5 (lower graph) sites. All decays are normalized to the intensity I_{ref} at NT_R = 0 as estimated from exponential fits to each data set, as shown in (a). The uncertainties result from the peak deconvolution and the normalization.

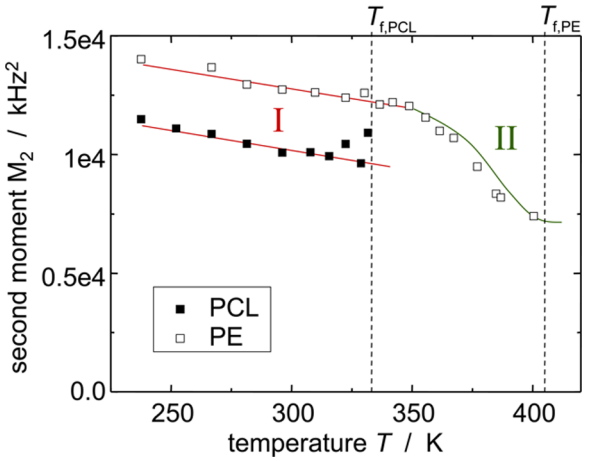

Figure 8. Second moment M_2 of the PCL-crystallite proton line shape, calculated from the FID fit parameters a and b (see Experimental Section), as a function of measurement temperature. For comparison, analogous data are shown for a melt-crystallized commercial HDPE sample.[30] The Roman numerals mark ranges of different temperature behavior, and the T_f denote the different melting temperatures.

removed by the proton decoupling is weaker for this site. This results in a lower sensitivity of the COO signal to decoupling imperfections and hence in a slower COO signal decay.[23] Moreover, as shown exemplarily in Figure 7b, the NT_R dependence of the methylene-carbon signal decay does not vary with temperature. Consequently, the decay does not originate from a thermally activated, dynamic process. Hence, chain dynamics in PCL crystallites on an intermediate time scale can so far be excluded from our data.

^{1}H Low-Field Measurements. *Second Moment of the Line Shape.* The second moment M_2 of the proton absorption line shape yields information about the average local homonuclear dipolar coupling that a proton "feels" within the sample.[31] As anisotropic chain motions within the PCL crystallites would cause a partial averaging of proton dipolar couplings when the motional rate exceeds the coupling strength of about 20 kHz,[41,42] they would lead to a reduction of the spectral line width and thus of M_2 as compared to the static case. This effect turns M_2 into an indicator for chain motions at rates larger than ~20 kHz.

Importantly, the proton spin system comprises intra- and interchain dipolar contacts. So even for the case where chain motion is mediated by 180° jumps, which leaves all so far discussed interaction tensor orientations unchanged and for instance ocurrs in the all-trans chain of crystalline polyethylene (PE), one can observe an effect due to the averaging of interchain couplings.[30] We thus include the ^{1}H low-field data to exclude the likely possibility of 180° jumps, noting again that the chains in PCL crystallites are also in an all-trans conformation.[16]

In Figure 8 the second moment values of the single broad PCL crystallite signal (corresponding the rapidly decaying initial part of the FID) are depicted as a function of measurement temperature over a wide temperature range and are compared to values for PE published previously.[30] The M_2 data were calculated according to $M_2 = a^2 + (b^2)/3$[32] from the fit parameters a and b deduced by fitting the (unrefocused) FID signals by means of the three-component fit model described in the Experimental Section. See Figure 4 for typical values of a and b. At increasing temperature, these values, and thus M_2, decay slightly and uniformly, likely as a result of thermal lattice expansion or very fast small-amplitude motions (vibrations and phonons),[5,43−45] which induce a slight decrease of the dipolar coupling strength due to increasing mean proton distances or some preaveraging, respectively.

In contrast, large-amplitude motions on an intermediate time scale cause an additional, stronger decay of M_2, as is seen for the case of PE.[30] The missing second decay in the case of PCL (note that it melts much earlier than PE) indicates that intermediate motions with rates in the range of some tens of kHz do not play a role in PCL crystallites. It is noted that the values for PCL are overall lower than the ones for PE, posing the question of a potential drop at lower temperatures. This can, however, safely be excluded on the basis of the crystallographic data for PCL.[16] Its orthorhombic unit cell (a = 7.496 Å, b = 4.974 Å, c = 17.297 Å) is very similar to the one of PE (a = 7.40 Å, b = 4.93 Å, c = 2.534 Å). Apart from the different c spacing that is trivially explained by the longer monomer unit, the unit cell is seen to be slightly expanded in the lateral direction, increasing the average interproton distances. The overall proton densities are calculated to about 31.0 and 43.3 H/nm^3 for PCL and PE, respectively. This easily explains the somewhat reduced second moment of PCL.

MSE Signal Loss. As a so-called time-reversing pulse sequence, the MSE sequence serves to refocus dipolar-dephased signals,[26,27] and we apply it here as an even more sensitive probe of possible weak changes in interchain proton dipolar couplings.[30] The dipolar refocusing proved to be almost quantitative in the case of PCL. However, compared to the unrefocused FID signals the MSE signals always show small phase-specific signal losses that we shall look at more closely. This refocusing inefficiency may have two

dx.doi.org/10.1021/ma401532v | Macromolecules 2013, 46, 7818−7825

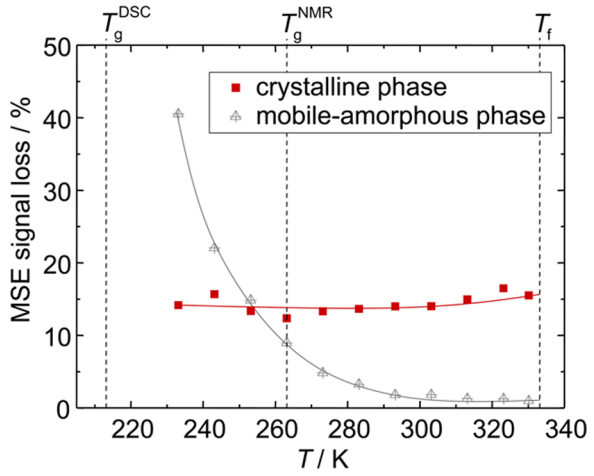

Figure 9. Phase-specific signal loss due to the action of the MSE sequence in the crystalline and mobile-amorphous phases of PCL as a function of the measurement temperature. The loss percentages were obtained by comparison of the respective signal intensities from fits to the MSE and the FID data. They are given relative to the mass (proton) fraction of the respective phases as derived from the FID data. The solid lines serve as guides to the eye, and T_f and T_g denote melting and glass transition temperatures of the crystalline and mobile phases, respectively.

possible origins:[30] (i) the occurrence of dynamics on an intermediate time scale (with rates k on the order of tens of kHz) which alters the strength of the homonuclear dipolar couplings during the pulse sequence and hampers a complete averaging of the couplings to zero at the end of the sequence and (ii) the occurrence of too large coupling strengths as compared to the inverse sequence length, resulting in a reduced efficiency of the pulse sequence with its finite cycle time.[29,46]

In Figure 9, the phase-specific MSE signal loss is depicted for PCL as a function of temperature between the glass transition and the melting point in relation to the corresponding signal contributions derived from the (unrefocused) FID signals. As is visible here, only a small, rather constant fraction of the crystallite signal is lost during the MSE sequence over the whole temperature range. By contrast, intermediate-regime motions within the PCL crystallites would lead to a very significant temperature dependence of the signal loss over a 1−2 decades broad range of motional rates, as previously observed for PE.[30] Hence, such dynamics can again be ruled out here. Rather, the signal loss results from imperfections due to strong dipolar couplings.

In comparison, and as a demonstration of the principle, for the MSE signal loss of the mobile-amorphous phase we in fact find a pronounced effect upon decreasing the temperature to around and below the "NMR glass transition" (see Figure 9), resulting from the slowdown of segmental motions to the intermediate time scale (tens of kHz), further accompanied by increasing dipolar coupling strengths upon entering the glassy state.

CONCLUSIONS

^{13}C high-field and ^{1}H low-field NMR experiments were performed at different temperatures for the semicrystalline polymer PCL in order to elucidate the crystalline-phase dynamics over a wide range of motional rates in detail. ^{13}C−^{1}H DIPSHIFT investigations provide evidence of fast, presumably vibrational motions of the C−H bonds in the methylene groups in PCL crystallites at rates higher than some hundreds of kilohertz, with amplitudes of up to 25°, growing with the distance to the COO groups. Moreover, ^{13}C CODEX data proved the absence of slow motions of the CSA tensors in the crystalline PCL chains with rates in the range of a few Hz to kHz.

Intermediate motions have also been investigated by means of ^{1}H low-field NMR experiments, focusing on possible changes in proton dipolar couplings between neighboring chains. This is necessary because we need to exclude the not unlikely possibility of symmetry-conserving 180° jumps of the all-trans chains of PCL. Neither the second-moment (M_2) data nor the MSE signal losses indicated dynamics in PCL crystallites on the intermediate time scale of about 1 kHz to 100 kHz over a wide temperature range of −40 °C up to the melting point at approximately 60 °C, in stark contrast to previous studies focusing on PE.

Besides, also the near-perfect signal refocusing for $t_1 = T_R$ in the ^{13}C−^{1}H DIPSHIFT curves and the equality and temperature independence of the NT_R-dependent decays of the CSA-CODEX reference intensities further confirmed the absence of slower, intermediate motions in the investigated temperature range of about 25−50 °C.

Our results stand in contrast to a conclusion of Kaji and Horii derived from ^{13}C CSA line shapes obtained from 2D SASS experiments,[15] according to which the CH_2 groups in the PCL chains perform intermediate to slow-regime dynamics with rates between 0.1 and 1 kHz within the crystallites. We can accommodate our findings with the data of Kaji and Horii by assuming that the narrowed CSA patterns measured by them for the central CH_2 groups either reflect the limit of fast dynamics in the crystallites or are due to *a priori* unknown, smaller CSA principal values. Reliable values would possibly have to be derived from quantum-chemical calculations based on the crystal structure rather than estimations based upon analogies. The increased line broadening observed by these authors may originate from the difficulties related to the dipolar decoupling from the methylene protons. We also note again that this earlier study was restricted to a single experimental temperature. As large-amplitude slow or intermediate-regime jump motions of chain parts within the PCL crystallites can thus be safely excluded, longer-range chain diffusion through the lamellae and lamellar thickening on cooling, as present in PE of linear topology,[47,48] is not expected for PCL. Hence, we conclude that a classification of PCL as a crystal-fixed polymer is justified.

AUTHOR INFORMATION

Corresponding Author

*E-mail: kay.saalwaechter@physik.uni-halle.de (K.S.).

Notes

The authors declare no competing financial interest.

ACKNOWLEDGMENTS

Funding of this work was provided by the Deutsche Forschungsgemeinsacht in the framework of the Sonderforschungsbereich SFB-TRR 102 (project A1). K. Schäler thanks the "Graduiertenförderung des Landes Sachsen-Anhalt" for her stipend. Infrastructural support from the European Union (ERDF programme) is gratefully acknowledged.

REFERENCES

(1) Schmidt-Rohr, K.; Spiess, H. W. *Multidimensional Solid-State NMR and Polymers*; Academic Press: London, 1994.

(2) Rault, J. *J. Macromol. Sci., Rev. Macromol. Chem. Phys.* **1997**, *C37*, 335−387.

(3) Hu, W.-G.; Schmidt-Rohr, K. *Acta Polym.* **1999**, *50*, 271−285.

(4) Mello, N. C.; Bonagamba, T. J.; Panepucci, H.; Dahmouche, K.; Judeinstein, P.; Aegerter, M. A. *Macromolecules* **2000**, *33*, 1280−1288.
(5) Olf, H. G.; Peterlin, A. *J. Polym. Sci., Part A-2: Polym. Phys.* **1970**, *8*, 771−789.
(6) McCall, D. W.; Douglass, D. C. *Appl. Phys. Lett.* **1965**, *7*, 12−14.
(7) Hu, W.-G.; Boeffel, C.; Schmidt-Rohr, K. *Macromolecules* **1999**, *32*, 1611−1619.
(8) Hu, W.-G.; Boeffel, C.; Schmidt-Rohr, K. *Macromolecules* **1999**, *32*, 1714.
(9) Schmidt-Rohr, K.; Spiess, H. W. *Macromolecules* **1991**, *24*, 5288−5293.
(10) Luo, C. F.; Sommer, J. U. *ACS Macro Lett.* **2013**, *2*, 31−34.
(11) Syi, J.-L.; Mansfield, M. L. *Polymer* **1988**, *29*, 987−997.
(12) Ito, M.; Kubo, M.; Tsuruta, A.; Tanaka, K. *J. Polym. Sci., Part B: Polym. Phys.* **1978**, *16*, 1435−1446.
(13) Woodruff, M. A.; Hutmacher, D. W. *Prog. Polym. Sci.* **2010**, *35*, 1217−1256.
(14) Semba, T.; Kitagawa, K.; Ishiaku, U. S.; Hamada, H. *J. Appl. Polym. Sci.* **2006**, *101*, 1816−1825.
(15) Kaji, H.; Horii, F. *Macromolecules* **1997**, *30*, 5791−5798.
(16) Bittiger, H.; Marchessault, R. H.; Niegisch, W. D. *Acta Crystallogr., Sect. B: Struct. Crystallogr. Cryst. Chem.* **1970**, *B 26*, 1923−1927.
(17) Hackel, C.; Zinkevich, T.; Belton, P.; Achilles, A.; Reichert, D.; Krushelnitsky, A. *Phys. Chem. Chem. Phys.* **2012**, *14*, 2727−2734.
(18) deAzevedo, E. R.; Saalwächter, K.; Pascui, O.; de Souza, A. A.; Bonagamba, T. J.; Reichert, D. *J. Chem. Phys.* **2008**, *128*, 104505.
(19) Fung, B. M.; Khitrin, A. K.; Ermolaev, K. *J. Magn. Reson.* **2000**, *142*, 97−101.
(20) Bielecki, A.; Kolbert, A. C.; Levitt, M. H. *Chem. Phys. Lett.* **1989**, *155*, 341−346.
(21) deAzevedo, E. R.; Hu, W.-G.; Bonagamba, T. J.; Schmidt-Rohr, K. *J. Am. Chem. Soc.* **1999**, *121*, 8411−8412.
(22) deAzevedo, E. R.; Hu, W.-G.; Bonagamba, T. J.; Schmidt-Rohr, K. *J. Chem. Phys.* **2000**, *112*, 8988−9001.
(23) Hackel, C.; Franz, C.; Achilles, A.; Saalwächter, K.; Reichert, D. *Phys. Chem. Chem. Phys.* **2009**, *11*, 7022−7030.
(24) Kricheldorf, H. R.; Berl, M.; Scharnagl, N. *Macromolecules* **1988**, *21*, 286−293.
(25) Wurm, A.; Zhuravlev, E.; Eckstein, K.; Jehnichen, D.; Pospiech, D.; Androsch, R.; Wunderlich, B.; Schick, C. *Macromolecules* **2012**, *45*, 3816−3828.
(26) Rhim, W.-K.; Pines, A.; Waugh, J. S. *Phys. Rev. Lett.* **1970**, *25*, 218−220.
(27) Pines, A.; Rhim, W.-K.; Waugh, J. S. *J. Magn. Reson.* **1972**, *6*, 457.
(28) Matsui, S. *Chem. Phys. Lett.* **1991**, *179*, 187−190.
(29) Fechete, R.; Demco, D. E.; Blümich, B. *J. Chem. Phys.* **2003**, *118*, 2411−2421.
(30) Bärenwald, R.; Champouret, Y.; Saalwächter, K.; Schäler, K. *J. Phys. Chem. B* **2012**, *116*, 13089−13097.
(31) Fedotov, V. D.; Schneider, H. Structure and Dynamics of Bulk Polymers by NMR-Methods. In *Structure and Dynamics of Bulk Polymers by NMR-Methods*; Diehl, P., Fluck, E., Günther, H., Kosfeld, R., Seelig, J., Eds.; Springer-Verlag: Berlin, 1989; Vol. *21*.
(32) Derbyshire, W.; van den Bosch, M.; van Dusschoten, D.; MacNaughtan, W.; Farhat, I. A.; Hemminga, M. A.; Mitchell, J. R. *J. Magn. Reson.* **2004**, *168*, 278−283.
(33) Abragam, A. *The Principles of Nuclear Magnetism*; Oxford University Press: Oxford, 1961.
(34) Schäler, K.; Ostas, E.; Schröter, K.; Thurn-Albrecht, T.; Binder, W. H.; Saalwächter, K. *Macromolecules* **2011**, *44*, 2743−âĂŞ2754.
(35) Levitt, M. H. In *Spin Dynamics - Basics of Nuclear Magnetic Resonance*, 2nd ed.; John Wiley & Sons, Ltd.: New York, 2008.
(36) Reichert, D.; Saalwächter, K. *Encycl. Nucl. Magn. Reson.* **2008**, DOI: 10.1002/9780470034590.emrstm1020.
(37) Wendoloski, J. J.; Gardner, K. H.; Hirschinger, J.; Miura, H.; English, A. D. *Science* **1990**, *247*, 431−436.
(38) Hirschinger, J.; Miura, H.; Gardner, K. H.; English, A. D. *Macromolecules* **1990**, *23*, 2153−2169.
(39) Cobo, M. F.; Achilles, A.; Reichert, D.; deAzevedo, E. R.; Saalwächter, K. *J. Magn. Reson.* **2012**, *221*, 85−96.
(40) Pines, A.; Abramson, E. *J. Chem. Phys.* **1974**, *60*, 5130−5131.
(41) Olf, H. G.; Peterlin, A. *J. Polym. Sci., Part A-2: Polym. Phys.* **1970**, *8*, 753−770.
(42) Ball, R. C.; Callaghan, P. T.; Samulski, E. T. *J. Chem. Phys.* **1997**, *106*, 7352−7361.
(43) Olf, H. G.; Peterlin, A. *Kolloid Z. Z. Polym.* **1967**, *215*, 97−111.
(44) Strobl, G. R.; Trzebiatowski, T.; Ewen, B. *Prog. Colloid Polym. Sci.* **1978**, *64*, 219−225.
(45) Hentschel, D.; Sillescu, H.; Spiess, H. W. *Makromol. Chem.* **1979**, *180*, 241−249.
(46) Hafner, S.; Demco, D. E.; Kimmich, R. *Solid State Nucl. Magn. Reson.* **1996**, *6*, 275−293.
(47) Albrecht, T.; Strobl, G. *Macromolecules* **1995**, *28*, 5827−5833.
(48) Strobl, G. *The Physics of Polymers: Concepts for Understanding Their Structures and Behavior*, 3rd ed.; Springer: Berlin, 2007.